

## Transport Properties in Drying of Solids\*

Aleksandra Sander, Jasna Prlić Kardum, Darko Skansi

Faculty of Chemical Engineering and Technology, University of Zagreb,  
Marulićev trg 19, 10000 Zagreb, Croatia, email: asander@pierre.fkit.hr

Congress paper

Received: 30. 1. 2001.

Accepted: 15. 3. 2001.

The transport properties in convection drying of industrially prepared roof tile clay slab were investigated on a laboratory scale in a temperature interval from 30 °C to 70 °C. The velocity and relative humidity of the drying air was kept constant.

Obtained drying data were approximated with different mathematical models. Applied models analysis enables evaluation of the main transport properties: effective diffusion coefficient, mass and heat transfer coefficients, thermal conductivity, drying constant, and exponential model parameters.

Based on Biot number value, the main transport mechanism was defined. Very small Biot numbers, less than 0.1, for both heat and mass transfer, indicates that the heat and mass transfer are externally controlled.

Evaluated parameters were connected with process condition and the drying constant. The air temperature strongly influences the drying kinetics, transport properties and exponential model parameters. Increase of temperature cause exponential increase of effective diffusion coefficient, thermal diffusivity and heat transfer coefficient, while values of parameter  $k$  and drying constant increases linearly. Exponential model parameter,  $n$ , is independent of temperature. It was found that the drying constant is essentially a combination of transport properties, transfer coefficients, geometry of the sample and experimental conditions.

*Key Words and Phrases:*

Convection drying, drying constant, heat transfer, mass transfer, transport properties

## Introduction

For a detailed description of the drying process, except knowing the drying kinetics, it is necessary to determine the influence of altering process conditions on essential process parameters (drying rate, process duration, transport properties).<sup>1,2</sup> The first step of this is to choose the mathematical model that describes process kinetics. The transport properties are estimated as parameters of the selected mathematical models by fitting it to experimental data. The main transport properties incorporated in most drying models are effective diffusion coefficient, mass and heat transfer coefficients, thermal conductivity and drying constant. Material moisture content and temperature, influence effective diffusion coefficient and effective thermal conductivity, while mass and heat transfer coefficients are functions of drying air characteristics and system geometry. The equilibrium material moisture content is a function of air humidity and temperature. On the other hand, drying constant depends on all mentioned properties (of air and material), and is a combination of the above transport properties.

Experimentally obtained data were correlated with several mathematical models:

1. II Fick's law (effective diffusion coefficient, mass transfer coefficient)<sup>1</sup> – **Model 1:**

$$\frac{\partial X}{\partial t} = \nabla(D_{\text{eff}} \nabla X) \quad (1)$$

with boundary conditions:

$$X(t=0, \delta) = X_0$$

$$\frac{\partial X(t, \delta=0)}{\partial \delta} = 0$$

$$\frac{\partial X(t, \delta=\pm l)}{\partial \delta} = \frac{k_m}{D_{\text{eff}}}(X(t, \delta=\pm l) - X_{\text{eq}})$$

2. Tomas&Skansi model (parameters  $k$  and  $n$ )<sup>3,4</sup> – **Model 2:**

$$X = (X_0 - X_{\text{eq}}) \cdot e^{-k \cdot t^n} + X_{\text{eq}} \quad (2)$$

3. Thin layer equation (drying constant)<sup>5,6</sup> – **Model 3:**

$$X = (X_0 - X_{\text{eq}}) \cdot e^{-K \cdot t^n} + X_{\text{eq}} \quad (3)$$

\*This article was presented as a poster at 14<sup>th</sup> International Congress of Chemical and process Engineering, CHISA 2000

4. II Fourier's law (thermal diffusivity, heat transfer coefficient)<sup>7,8</sup> – **Model 4:**

$$\frac{\partial T}{\partial t} = \nabla(a\nabla T) \quad (4)$$

with boundary conditions:

$$\begin{aligned} T(t=0, \delta) &= T_0 \\ \frac{\partial T(t, \delta=0)}{\partial \delta} &= 0 \\ \frac{-\partial T(t, \delta=\pm l)}{\partial \delta} &= \frac{h_H}{\lambda} (T(t, \delta=\pm l) - T_{\text{eq}}) - \\ &\quad -\Delta h_s \frac{k_m}{\lambda} (X_{\text{eq}} - X(t, \delta=\pm l)) \end{aligned}$$

Proposed model parameters ( $k$ ,  $n$ ) and transport properties ( $D_{\text{eff}}$ ,  $a$ ,  $h_M$ ,  $h_H$ ) are determined by regression analysis. To test the fitting of experimental data to the model, the mean square deviation has been used.

$$\begin{aligned} \sigma_x &= \frac{1}{n} \sum_i \left( \frac{X_{i,\text{calc}} - X_i}{x_i} \right)^2 \\ \sigma_T &= \frac{1}{n} \sum_i \left( \frac{T_{i,\text{calc}} - T_i}{T_i} \right)^2 \end{aligned} \quad (5)$$

A two-parameter exponential model (Tomas&Skansi) successfully describes drying kinetics of many materials (carrot, potato, bean, paper, clay, some pharmaceutical materials). Model parameters,  $k$  and  $n$ , are function of process conditions, material properties and dominant transfer mechanism.

Criterion for determination of rate controlling mechanism of mass and heat transfer was Biot number<sup>1,7</sup>:

$$\begin{aligned} Bi_m &= \frac{k_m \delta}{D_{\text{eff}}} \\ Bi_H &= \frac{k_m \delta}{\lambda} \end{aligned} \quad (6)$$

Given boundary conditions (Model\_1 and Model\_4) assumed that there are significant external resistances to heat and mass transfer. If Biot number is smaller than 0.1, drying process is externally controlled<sup>1,7,8</sup>, which means that internal resistance to mass and heat transfer is negligible. In the case of porous materials with large pores and for thin plates, the condition  $Bi < 1$  is often fulfilled. At small Biot numbers the surface temperature and the moisture content differs little from the temperature and the moisture content in the center of the slab. This results with uniform distribution of temperature and moisture across the slab.

## Theoretical estimation of heat and mass transfer coefficient

In estimating drying rates, the use of heat transfer coefficients is preferred because they are usually more reliable than mass transfer coefficient. When mass transfer coefficient is calculated from drying experiment, the partial pressure is usually determined from the measured surface temperature. Small errors in temperature cause relatively large errors in partial pressure and hence in the mass transfer coefficient. For many cases in drying, the heat transfer coefficient can be expressed as:

$$h_H = \frac{\alpha \cdot G_m^\beta}{D_c^\delta} \quad (7)$$

where:  $\alpha$ ,  $\beta$ ,  $\gamma$  are empirical constants,  $G_m$  is mass flow rate of air in  $\text{kg m}^{-2} \text{s}^{-1}$ , and  $D_c$  is characteristic dimension of the system<sup>9</sup>.

For flow parallel to plane plate<sup>1,10</sup>, in the absence of applicable specific data, heat transfer coefficient can be estimated as:

$$h_H = 0.0204 \cdot G_m^{0.8} \quad (8)$$

or

$$h_H = 0.01 \cdot G_m^{0.8} \quad (9)$$

To obtain mass transfer data the analogy of heat and mass transfer can be used. In air conditioning processes, in the constant rate period, the heat and mass transfer analogy is usually expressed by the Lewis relationship<sup>1,9,10,11</sup>.

$$\frac{h_H}{h_G} = c_p \quad (10)$$

where  $h_G$  is the film mass transfer coefficient equal to  $h_M \cdot \rho_{\text{air}}$  in  $\text{kg m}^{-2} \text{s}^{-1}$ , and  $c_p$  is the specific heat of hot air in  $\text{J kg}^{-1} \text{K}^{-1}$ .

Since the drying process is also affected by the internal heat and moisture diffusivities during the falling rate period, the heat and mass transfer coefficient on the gas side changes owing to the continuous decrease in vapor diffusivity of the material in the surface layer.

## Material and methods

Thin plates of illit-montmorillonit clay ( $\rho_m = 2373 \text{ kg m}^{-3}$ ) with dimensions  $65 \times 55 \times 2 \text{ mm}$ , were cut from a raw industrially shaped, flat roof tile. Until exposing the samples to hot airflow, they were kept in hermetically closed containers. Initial moisture content was 18% (wet basis).

The laboratory analysis<sup>12</sup> of raw materials used for the production of tiles, shows that clay contains the mineral quartz, kaolin, feldspat and iron hydroxides. The clay gives 1.4 to 6.1 % of the residue on a sieve of  $10^4$  holes/cm<sup>2</sup>, and 30% of particles are smaller than  $2 \mu\text{m}$ . The point at which clinkering appears is  $1048 \text{ }^\circ\text{C}$ , the sintering point is at  $1100 \text{ }^\circ\text{C}$ , and the baking temperature is  $930$  to  $950 \text{ }^\circ\text{C}$ . The shrinkage caused by drying is 7 to 8 %, which points to the significant sensitiveness of that clay while drying.

Pore size distribution is determined by the adsorption of nitrogen within the material on the ASAP 2000 system. Pore size analysis gives cumulative adsorption surface area of  $32.46 \text{ m}^2 \text{ g}^{-1}$ , cumulative adsorption pore volume of  $0.05276 \text{ cm}^3 \text{ g}^{-1}$ , micropore volume of  $0.000867 \text{ cm}^3 \text{ g}^{-1}$ , and average pore diameter of  $65.013 \text{ \AA}$ . The porosity of the illit-montmorillonit clay is 0.111.

Equilibrium material moisture content at given temperatures was determined from sorption isotherms<sup>12</sup>.

## Experimental setup

Measurements were carrying out in the convection drier shown on Figure 1. The superficial air velocity, with relative humidity of 67%, had a constant value of  $0.43 \text{ m s}^{-1}$ . Experiments were performed at different air temperatures:  $30 \text{ }^\circ\text{C}$ ,  $40 \text{ }^\circ\text{C}$ ,  $50 \text{ }^\circ\text{C}$ ,  $60 \text{ }^\circ\text{C}$  and  $70 \text{ }^\circ\text{C}$ . During drying process, the change of mass and temperature of the wet sample were continuously measured. Two identical samples were used for the experiment, one to measure the mass, and the other to measure the temperature during drying. The sample used for measuring the mass, was hanged on the extension of a digital balance with precision of  $\pm 0.01 \text{ g}$ . One side of the thermocouple, used for measuring the temperature, was firmly leant against the surface of the parallel sample. It was shown earlier, even for a sample with dimensions  $138 \times 65 \times 16 \text{ mm}$ , that there are no temperature gradient within material<sup>12</sup>.

## Results and discussion

Convection drying of thin industrially prepared illit-montmorillonit clay plate has been performed in the range of hot air temperature from  $30 \text{ }^\circ\text{C}$  to  $70 \text{ }^\circ\text{C}$ . Relative humidity (67%) and superficial drying air velocity ( $0.43 \text{ m s}^{-1}$ ) maintained at the same value for all experiments.

Typical drying curves (normalized material moisture content and temperature vs. time) are shown on Figure 2. Increase of air temperature re-

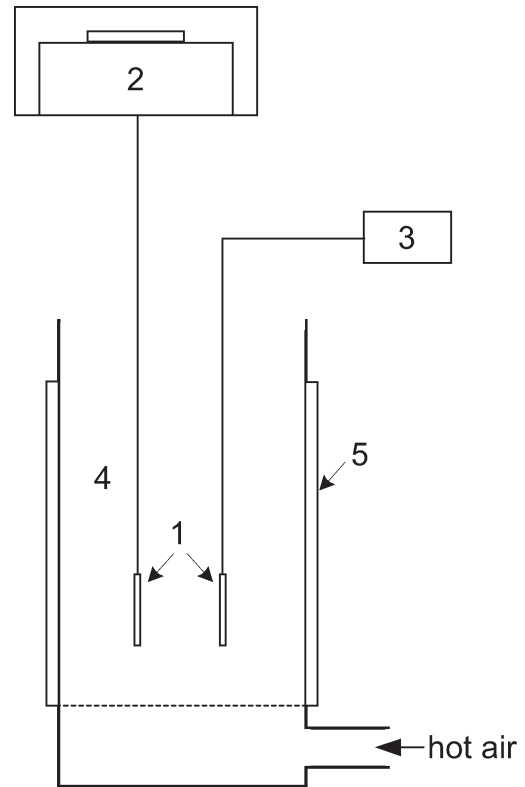


Fig. 1 – Scheme of the laboratory test device for convective drying

1 – samples; 2 – digital balance; 3 – digital thermometer; 4 – dryer chamber; 5 – insulation

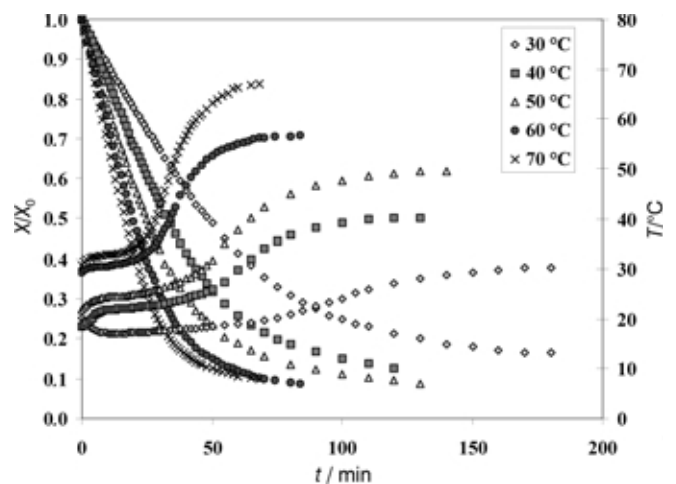


Fig. 2 – Dependence of dimensionless material moisture content and temperature vs. drying time for convective drying of clay

sults in steepest functional dependence ( $X(t)/X_0$ ) (higher drying rates), reducing the drying time.

As mentioned above, all applied mathematical models involve material equilibrium moisture content, so it was necessary to determine its values. Equilibrium moisture content was determined by means of sorption isotherms for a given material. Equilibrium moisture content exponentially de-

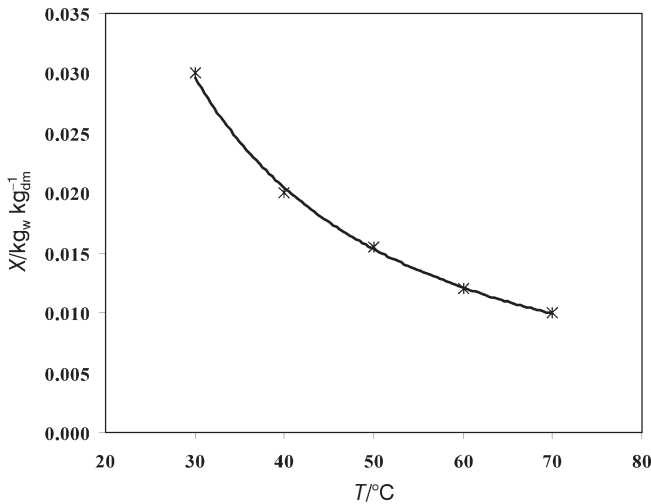


Fig. 3 – Equilibrium moisture content for illit-montmorillonit clay

depends on drying temperature, Figure 3. Lower values correspond to higher temperature, which was anticipated for reason that the relative humidity of air remains constant.

In order to find out which of applied models better correlates experimental data, parallel survey of measured and calculated data (all selected models), at air temperature of 70 °C, is show on Figure 4. The best correlation for mass transfer is achieved with Tomas&Skansi model, although all models are compatible with the experimental data. II Fick'law (Model\_1) and thin layer equation (Model\_3) are used to evaluate effective diffusion coefficient, mass transfer coefficient and the drying constant. Mathematical model,  $T(t)$ , for heat transfer also correlates highly with measured material temperature.

Predicted values of heat transfer coefficient are evaluated by following algorithm:

– drying coefficient on partial pressure basis,  $h_p$  is evaluated from experimentally obtained constant drying rate,  $R_c$

$$h_p = \frac{R_c}{(p_s - p_v)}$$

– a dynamic equilibrium between the rate of heat supply and the rate of moisture removal in the constant-rate period can be represented as follows:

$$R_c = \frac{h_H \cdot (T_G - T_s)}{\Delta H_s} = h_p \cdot (p_s - p_v) = h_p \cdot \Delta p_{lm} \cdot (Y_s - Y_G) = h_Y \cdot (Y_s - Y_G)$$

– with obtained values of heat transfer coefficient, mass transfer coefficient is evaluated by equation 10.

Those equations assume that both the drying gas and vapor behave as perfect gases and that radiation and conduction to and from the evaporating surface are negligible. These assumptions holds when the conditions in the drying gas are not very different from those in the solid being dried. As mentioned before, during the falling rate period, drying process is also affected by the internal heat and moisture diffusivities so the heat and mass transfer coefficient on the gas side changes. Owing to that reasons there are differences between predicted and evaluated, from mathematical models, values for both heat and mass transfer coefficient. Predicted values of heat transfer coefficient ranges from 0.047 to 0.120 W m<sup>-1</sup> °C<sup>-1</sup>, while predicted values of mass transfer coefficient ranges from 1.78 · 10<sup>-7</sup> to 1.9 · 10<sup>-6</sup> m s<sup>-1</sup>. Equations 8 and 9 are not suitable for this case.

The influence of drying condition (hot air temperature) on approximated values of transport properties, and parameters  $k$  and  $n$  are presented on Figures 5 to 8. Increase of temperature cause exponential increase of effective diffusion coefficient, thermal conductivity, heat transfer coefficients and parameter  $k$ , while mass transfer coefficient and dry-

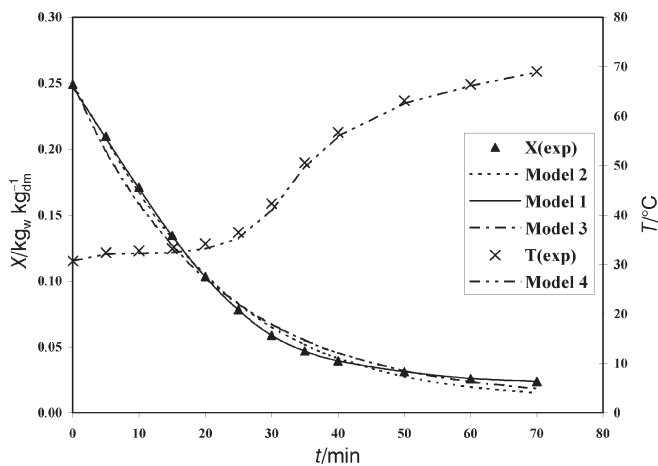


Fig. 4 – Comparison of mathematical models and experimental data

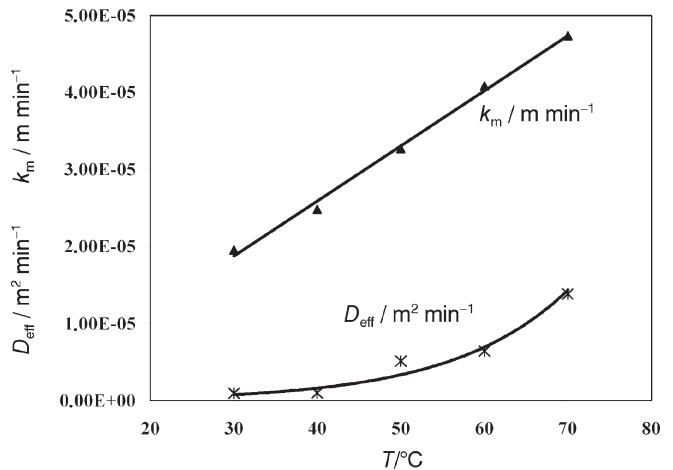


Fig. 5 – The influence of drying temperature on effective diffusion coefficient and mass transfer coefficient

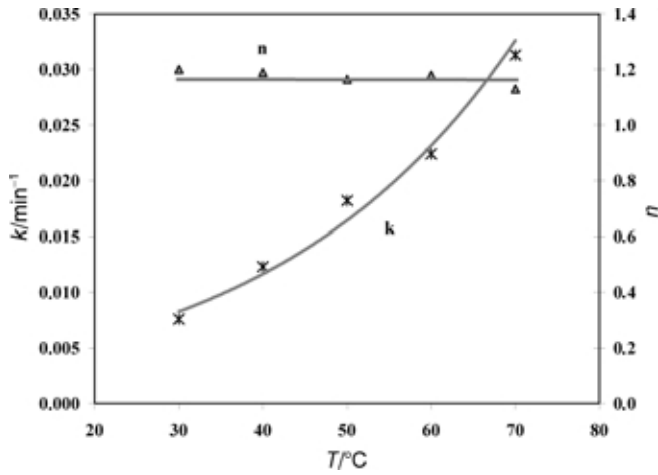


Fig. 6 – Parameters  $k$  and  $n$  vs. drying temperature

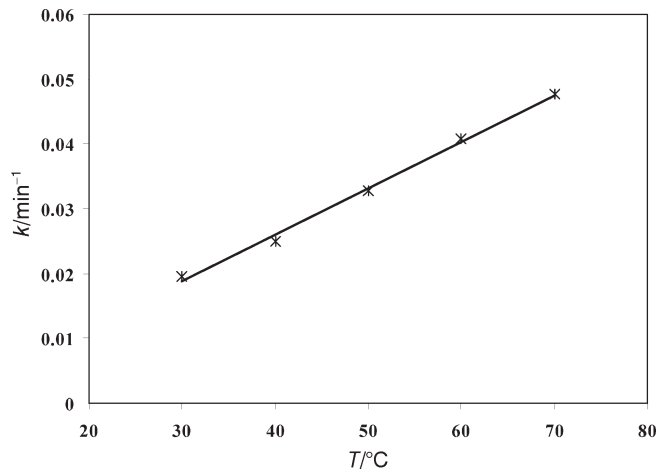


Fig. 7 – Dependence of drying constant of drying temperature

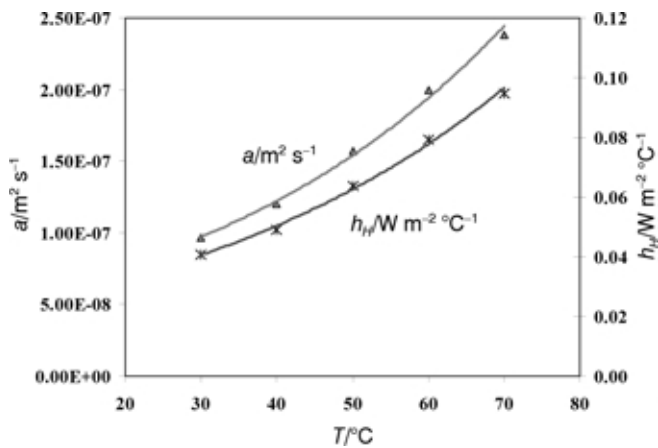


Fig. 8 – Thermal diffusivity and heat transfer coefficient as a function of drying temperature at given process condition ( $v, \phi$ )

ing constant increases linearly. Parameter  $n$  is independent of temperature. Exponential dependencies of the above parameters are probably caused by the exponential temperature dependence of vapor pressure inside materials (Antoine Reid correlation). It was shown earlier that value of parameter  $n$  depends on the way that heat is supplied to a material (drying method)<sup>13</sup>.

Relations between the drying constant and determined coefficients are shown on Figure 9. That attempt was made because the drying constant includes all the transport properties in a simple exponential equation. Increase of thermal conductivity, heat and mass transfer coefficients and parameter  $k$ , cause linear increase of drying constant. Dependence between drying constant and effective diffusion coefficient is not linear. That is in concordance with assumption that the mass transfer is not internally controlled (if the controlling mechanism is the moisture diffusion in the slab, then the value of effective diffusion coefficient must linearly depends on drying constant).

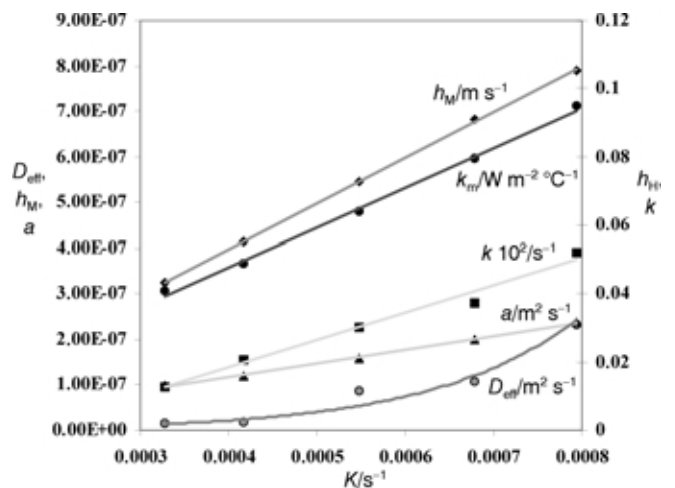


Fig. 9 – Relations between the drying constant and determined transfer coefficients

Obtained Biot numbers, for both mass and heat transfer, are very small ( $Bi_M$  ranges from  $3.42 \cdot 10^{-3}$  to  $2.12 \cdot 10^{-2}$ ;  $Bi_H$  from  $1.4 \cdot 10^{-4}$ – $1.5 \cdot 10^{-4}$ ). The surface temperature and moisture content differs little from its value at the center of the slab, so temperature and moisture distribution across the material is uniform. The rate of heating and dehumidification depends only on the intensity of heat and mass transfer at the solid/air interface, so the process of mass and heat transfer is externally controlled. To substantiate that, resistance to heat and mass transfer are shown on Figures 10 and 11. It can be seen that external resistances,  $1/h_M$  and  $1/h_H$ , are much larger than internal resistances,  $L/\lambda$  and  $L/D_{eff}$ .

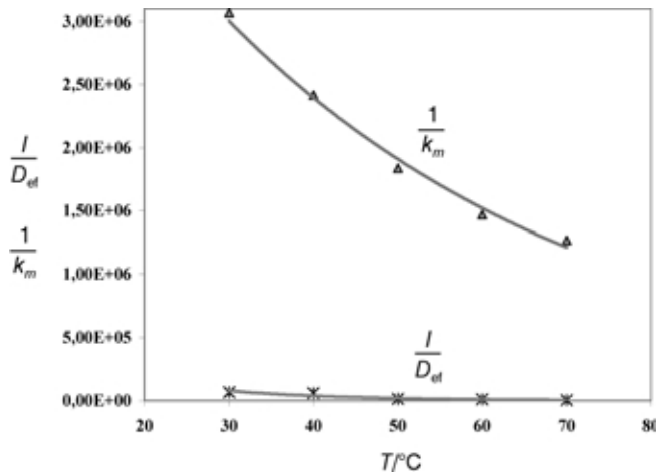


Fig. 10– Dependence between mass transfer resistance vs. drying temperature

## Conclusion

In order to estimate transport properties of thin industrially prepared clay plate, kinetics of isothermal convection drying were investigated in temperature interval from 30 °C to 70 °C, on a laboratory scale

High correlation between experimental and calculated data justifies the applied mathematical models for describing the drying kinetics in isothermal conditions.

The main transport properties of thin clay plate: effective diffusion coefficient, mass and heat transfer coefficients, thermal conductivity, drying constant, and exponential model parameters in isothermal condition, were estimated.

Very small Biot numbers, less than 0.1, for both heat and mass transfer, indicates that the heat and mass transfer are under external conditions.

The influence of air temperature on the drying kinetics, transport properties and exponential model parameters was analyzed. Increase of temperature cause exponential or linear increase of all mentioned coefficients, except exponential model parameter,  $n$ , that is independent of temperature.

It was found that the drying constant is essentially combination of transport properties, transfer coefficients, geometry of the sample and experimental conditions. Dependencies between drying constant and evaluated transport properties, except effective diffusion coefficient, are linear.

## Notation

- $a$  – thermal diffusivity,  $\text{m}^2 \text{s}^{-1}$
- $Bi$  – Biot number
- $D_{\text{eff}}$  – effective moisture diffusion coefficient,  $\text{m}^2 \text{s}^{-1}$
- $G$  – mass flow rate,  $\text{kg s}^{-1} \text{m}^{-2}$
- $h_G$  – mass transfer coefficient,  $\text{kg m}^{-2} \text{s}^{-1}$
- $h_H$  – heat transfer coefficient,  $\text{W m}^{-2} \text{K}^{-1}$

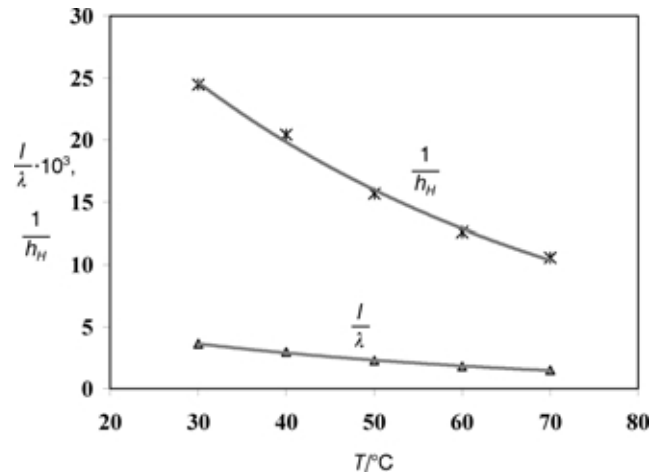


Fig. 11– Dependence between heat transfer resistance vs. drying temperature

- $h_M$  – mass transfer coefficient,  $\text{m s}^{-1}$
- $h_p$  – mass transfer coefficient,  $\text{kg m}^{-2} \text{s}^{-1} \text{Pa}^{-1}$
- $h_Y$  – mass transfer coefficient on humidity basis,  $\text{kg s}^{-1} \text{m}^{-2} (\text{kg}_w/\text{kg}_a)$
- $\Delta H$  – latent heat of evaporation,  $\text{J kg}^{-1}$
- $k$  – parameter in model 2,  $\text{s}^{-1}$
- $L$  – half thickness of a slab,  $\text{m}$
- $K$  – drying constant,  $\text{s}^{-1}$
- $n$  – parameter in model 2
- $p$  – partial pressure,  $\text{Pa}$
- $R$  – drying rate,  $\text{kg/m}^2\text{s}$
- $t$  – time,  $\text{s}$
- $T$  – temperature,  $^{\circ}\text{C}$
- $x$  – slab thickness,  $\text{m}$
- $X$  – moisture content,  $\text{kg}_w/\text{kg}_{\text{dm}}$

## Greek Symbols:

- $\alpha$  – constant
- $\beta$  – constant
- $\delta$  – constant
- $\lambda$  – thermal conductivity,  $\text{W m}^{-1} \text{K}^{-1}$
- $\rho$  – density,  $\text{kg m}^{-3}$
- $\sigma$  – mean square deviation

## Index:

- $a$  – air
- $c$  – constant rate
- $dm$  – dry material
- $eq$  – equilibrium
- $h$  – heat
- $M$  – mass
- $m$  – material
- $s$  – saturation
- $v$  – vapor
- $w$  – water
- $0$  – initial

**References**

1. *Mujumdar, A. S.*, Handbook of Industrial Drying, Vol. 1, Part I, Marcel Dekker, Inc., New York, 1995.
2. *Sattler, K., Feindt, H. J.*, Thermal Separation Processes, VCH, Weinheim, 1995, 317
3. *Tomas, S., Skansi, D., Sokele, M.*, Drying Technology **11** (1993) 1353–1369.
4. *Sander, A., Tomas, S., Skansi, D.*, Drying Technology **16** (1998) 1487–1499,
5. *Jayas, D.S.* et al., Drying Technology, **9** (1991) 551–588.
6. *Sokhansany, S., Genkowski, S.*, in proc. 6<sup>th</sup> Inter. Drying Symp. (IDS 1988), Versailles, France '88, 159–170.
7. *Isachenko, V. P., Osipova, V. A., Sukomel, A. S.*, Heat Transfer, MIR Publishers, Moscow, 1977.
8. *Sissom, L. E., Pitts, D. R.*, Elements of Transport Phenomena, McGraw Hill Book Company, New York, 1972.
9. *Perry, R. H., Chilton, C. H., Kirkpatrick, S. D.*, Chemical Engineers Handbook, McGrawHill Book Company, Inc., N. York, 1963.
10. *Nonhebel, G., Moss, A. A. H.*, Drying of Solids in the Chemical Industries, Butterworth&Co., Ltd., 1971.
11. *Toei, R.*, Drying Technology, **14** (1996) 1–194
12. *Tomas, S.*, Untersuchung der Trockungskinetik der Ziegeleerzeugnisse, Master Thesis, University of Zagreb, 1988.
13. *Prlić Kardum, J., Sander, A., Skansi, D.*, Drying Technology, **19** (2001) 169–185.

